NATIONAL ADVISORY COMMITTEE FOR AERONAUTICS

TECHNICAL NOTE 2775

EFFECT OF LINEAR SPANWISE VARIATIONS OF TWIST AND CIRCULAR-ARC CAMBER ON LOW-SPEED STATIC STABILITY, ROLLING, AND YAWING CHARACTERISTICS OF A 45° SWEPTBACK WING OF ASPECT RATIO 4 AND TAPER RATIO 0.6

By Byron M. Jaquet

Langley Aeronautical Laboratory
Langley Field, Va.

Washington

August 1952

1U

NATIONAL ADVISORY COMMITTEE FOR AERONAUTICS

TECHNICAL NOTE 2775

EFFECT OF LINEAR SPANWISE VARIATIONS OF TWIST AND CIRCULAR-ARC CAMBER ON LOW-SPEED STATIC STABILITY, ROLLING, AND YAWING CHARACTERISTICS OF A 45° SWEPTBACK WING OF ASPECT RATIO 4 AND TAPER RATIO 0.6

By Byron M. Jaquet

SUMMARY

An investigation at low scale has been made in the Langley stability tunnel in order to determine the effect of linear spanwise variations of twist and circular-arc camber on the low-speed aerodynamic characteristics and static-stability and rotary-stability (rolling and yawing) derivatives of a wing of aspect ratio 4, taper ratio 0.6, and with 45° sweepback of the quarter-chord line.

Results of the investigation indicate that twist or camber produced only small changes in the maximum lift coefficient. A combination of camber and twist was more effective than twist alone in providing an increase in the maximum lift-to-drag ratio in the moderate lift-coefficient range for the wings investigated. The variation of static longitudinal stability through the lift-coefficient range was less for the twisted wing than for the twisted and cambered or plane wing.

A combination of twist and camber generally extended the initial linear range of several of the static- and rotary-stability derivatives to a higher lift coefficient and, although these effects were small, higher Reynolds numbers may result in larger effects.

INTRODUCTION

One of the disadvantages encountered in the use of sweptback wings is the premature stall of the tip region which causes the variations of the aerodynamic parameters to depart from their initial linear trends at low angles of attack (refs. 1 and 2). These nonlinearities often lead to difficulty in dynamic stability. Twist, camber, or a combination of the two is sometimes incorporated in swept wings in order to provide a

more satisfactory spanwise load distribution. These factors would also be expected to extend the initial linear range of those parameters dependent primarily on the spanwise load distribution of the wing to higher angles of attack.

The effect of linear spanwise variations of twist and a combination of twist and circular-arc camber on the low-speed static-stability and rotary-stability derivatives (rolling and yawing) of a wing with 45° sweepback of the quarter-chord line, an aspect ratio of 4, and a taper ratio of 0.6 were determined in this investigation. An indication of the effect of camber was attained by a comparison of the data for the twisted wing with that for the twisted and cambered wings. Also included was the determination of the effect of leading-edge roughness on the aerodynamic characteristics of the wings at zero angle of sideslip.

The present investigation is a part of a research program being made in the Langley stability tunnel in order to determine the effect of various geometric parameters on the static- and rotary-stability derivatives of wings and airplane configurations.

SYMBOLS

The system of stability axes, with the origin at the projection of the quarter-chord point of the mean aerodynamic chord on the plane of symmetry, is used throughout the paper. The positive directions of the forces, moments, and angular displacements are shown in figure 1. The symbols and coefficients used herein are defined as follows:

A	aspect ratio, b^2/S
b	wing span, ft
S	wing area, sq ft
c	local chord parallel to plane of symmetry, ft
$\bar{c}$	mean aerodynamic chord, $\frac{2}{S}\int_0^{b/2} c^2 dy$, ft
c_r	root chord, ft
c_t	tip chord, ft
λ	taper ratio, c_t/c_r

y	spanwise distance measured from, and perpendicular to, plane of symmetry, ft
α	angle of attack of root-chord line, deg
ϵ	angle of twist about 50-percent-chord line, measured with respect to root-chord line and in a plane parallel to plane of symmetry, deg; positive when trailing edge is down
θ	camber angle, angle between chord line and line tangent to mean camber line at 75-percent-chord point, deg
ϵ_e	effective twist angle, $\epsilon + \theta$, deg
Λ	angle of sweepback of quarter-chord line, deg
β	angle of sideslip, deg
Ψ	angle of yaw, deg
V	free-stream velocity, fps
ρ	mass density of air, slugs/cu ft
r	yawing angular velocity, radians/sec
p	rolling angular velocity, radians/sec
$\frac{rb}{2V}$	lateral flight-path curvature, radians
$\frac{pb}{2V}$	wing-tip helix angle, radians
C_L	lift coefficient, $\frac{\text{Lift}}{\frac{\rho}{2}V^2S}$
C_D	drag coefficient, $\frac{D}{\frac{\rho}{2}V^2S}$
C_Y	lateral-force coefficient, $\frac{Y}{\frac{\rho}{2}V^2S}$
C_m	pitching-moment coefficient, $\frac{M}{\frac{\rho}{2}V^2S\bar{c}}$

C_l rolling-moment coefficient, $\frac{M}{\frac{\rho}{2}V^2Sb}$

C_n yawing-moment coefficient, $\frac{N}{\frac{\rho}{2}V^2Sb}$

D drag, lb

Y lateral force, lb

M pitching moment, ft-lb

L rolling moment, ft-lb

N yawing moment, ft-lb

L/D ratio of lift to drag

$C_{L_\alpha} = \frac{\partial C_L}{\partial \alpha}$

$C_{l_\beta} = \frac{\partial C_l}{\partial \beta}$

$C_{n_\beta} = \frac{\partial C_n}{\partial \beta}$

$C_{Y_\beta} = \frac{\partial C_Y}{\partial \beta}$

$C_{l_p} = \frac{\partial C_l}{\partial \frac{pb}{2V}}$

$C_{n_p} = \frac{\partial C_n}{\partial \frac{pb}{2V}}$

$C_{Y_p} = \frac{\partial C_Y}{\partial \frac{pb}{2V}}$

$$C_{l_r} = \frac{\partial C_l}{\partial \frac{rb}{2V}}$$

$$C_{n_r} = \frac{\partial C_n}{\partial \frac{rb}{2V}}$$

$$C_{Y_r} = \frac{\partial C_Y}{\partial \frac{rb}{2V}}$$

Subscript:

l local

APPARATUS, MODELS, AND TESTS

The 6-foot-diameter rolling-flow test section (ref. 3) and the 6- by 6-foot yawing-flow test section (ref. 4) in which rolling or yawing flight is simulated by rolling or curving the air stream about a model attached to a support strut were used for the present investigation in the Langley stability tunnel. The support strut was rigidly attached to a six-component balance system.

Three wings (constructed of laminated mahogany and given highly polished surfaces) having identical plan forms but differing in the amounts of twist or camber were used in the present investigation. (See fig. 2.) The basic airfoil profile used was the NACA 65A008 section in planes parallel to the plane of symmetry. Geometric details of the wings are shown in figure 2 wherein each wing is assigned an identifying number. Wing 1 had 0° twist and camber and is referred to hereinafter as the plane wing. Each semispan of wing 2 was given -6° twist at the tip about the 50-percent-chord line parallel to the plane of symmetry, and the twist decreased linearly from -6° at the tip to 0° at the root section (-6° twist was chosen to provide an elliptic spanwise loading at $C_L = 0.6$). Wing 3 had the same twist distribution as wing 2 and in addition had circular-arc camber with a camber angle which varied linearly from 3° at the tip to 0° at the plane of symmetry. The effective twist of wing 3 at the tip (combined twist and camber) was -3°. The variations of twist and effective twist across the semispans of wings 2 and 3 are shown in figure 3. Ordinates for the airfoil sections are given in table I.

The four types of tests made with each wing are indicated in table II along with pertinent test conditions. The wings were tested over a small Reynolds number range $\left(0.565 \times 10^6 \text{ to } 1.14 \times 10^6\right)$ at $\beta = 0^\circ$, $\frac{pb}{2V} = 0$, and $\frac{rb}{2V} = 0$. However, only minor changes in the longitudinal characteristics resulted and, hence, the data are not presented herein.

Transition strips, composed of cellulose tape impregnated with fine carborundum particles, were attached along the leading edge of the wings from 0 to 0.05 of the local chord for a few tests at $\beta = 0^\circ$, $\frac{pb}{2V} = 0$, and $\frac{rb}{2V} = 0$.

CORRECTIONS

Approximate jet-boundary corrections derived for unswept wings were applied to the angle of attack and the drag coefficient. A correction was applied to C_{Y_r} to account for the pressure gradient associated with yawing flow. (See ref. 4.)

The effect of the support strut on C_L, C_D, and C_m was determined for wing 1 and the tares determined were applied to all three wings (fig. 4).

RESULTS AND DISCUSSION

Static Longitudinal Characteristics

Lift characteristics.- Application of a linear spanwise variation of twist or a combination of twist and circular-arc camber did not affect the lift-curve slope of the wing (fig. 5) at $C_L = 0$. Twist or effective twist (combined twist and camber) produced a change in the angle of zero lift which would be expected and, consequently, in lift coefficient at zero angle of attack. Zero lift occurred at about 0° angle of attack for the plane wing, whereas application of linear twist increased the angle of attack for zero lift to about 2.4°. Incorporation of camber, in addition to twist, reduced the angle of attack for zero lift to about 1.5°. These trends are as would be expected inasmuch as the average effective angle of twist of wing 2 was -3° and that of wing 3 was -1.5°.

The use of twist or twist and camber produced only small changes in maximum lift coefficient at the Reynolds number of this investigation

(Reynolds number = 0.895×10^6). Larger changes in the maximum lift coefficient due to twist or camber may occur at higher Reynolds numbers.

Drag characteristics.- In the low lift-coefficient range, twist or camber had no measurable effects on the drag coefficient (fig. 5); however, at moderate and high lift coefficients, twist increased the drag considerably. Addition of 3° of camber to the twisted wing almost canceled this increase.

Wing 3 had the highest value of L/D (fig. 6), whereas wing 2 had only a slightly higher value of L/D than the plane wing (wing 1). Wing 3 maintained a value of L/D higher than that of the other wings throughout the moderate lift-coefficient range.

A rapid rise in the expression $C_D - \frac{C_L^2}{\pi A}$ (fig. 6) has frequently been used as an indication of the lift coefficient at which separation effects become evident and, thus, the slopes of curves of derivatives are likely to change. A small increase in the lift coefficient where a rapid rise in $C_D - \frac{C_L^2}{\pi A}$ occurs was noted for the twisted and cambered wing.

Pitching-moment characteristics.- Twist caused a large positive increment in the pitching-moment coefficient (due to a forward and inboard movement of the center of pressure) through most of the lift-coefficient range, whereas camber, as indicated by a comparison of wings 2 and 3, caused a negative increment (due to a rearward and outboard movement of the center of pressure) which was large at low lift coefficients and decreased as the lift coefficient increased (fig. 5). The variation of stability through the lift-coefficient range was less for the twisted wing than for the plane or twisted and cambered wing.

Effect of transition strips.- A comparison of figures 5, 6, 7, and 8 shows that fixing the transition at the leading edge of the wing decreased the maximum lift coefficient and the maximum value of L/D and caused an increase in the value of C_D at low lift coefficients. The maximum lift coefficient of wings 2 and 3 was more sensitive to the roughness along the leading edge; this fact indicates that these wings might be more sensitive to an increase in Reynolds number.

Fixing transition at the wing leading edge caused a forward movement of the aerodynamic center for each wing, as is evident from the change in slope of C_m plotted against C_L. (Compare figs. 5 and 7.)

Static Lateral Stability Characteristics

Twist and camber had insignificant effects on the variation of C_{Y_β} and C_{n_β} with C_L (fig. 9).

The variation of C_{l_β} with C_L (fig. 9) for the plane wing is linear up to about the same lift coefficient as that at which there is a rapid rise in $C_D - \frac{C_L^2}{\pi A}$ with increase in C_L (fig. 6). Incorporating a linear twist variation had little effect on the linear range of the curve of C_{l_β} plotted against C_L. Combining camber with twist extends the linear range of the curve by about $C_L = 0.10$. It should be noted that the test Reynolds number was low (0.895×10^6) and that perhaps greater effects of twist or camber would be realized at higher Reynolds numbers.

Twist and camber had essentially no effect on the value of C_{l_β} at low lift coefficients. The addition of camber to the twisted wing caused a large increase in the value C_{l_β} at moderate and high lift coefficients; hence, it was indicated that the camber in wing 3 caused the load near the tips to be retained at higher angles of attack than for wings 1 or 2. The increments in C_{l_β} in the moderate lift-coefficient range due to twist or camber are larger than the increments caused by adding one of several vertical tails to a wing-fuselage combination having the same wing as wing 1. (See ref. 5.)

Figure 10 is included to illustrate the variation of C_Y, C_n, and C_l with β for angles of sideslip greater than those ($\beta = \pm 5^\circ$) used to determine C_{Y_β}, C_{n_β}, and C_{l_β}. The lift coefficients for each wing are different for a given angle of attack.

Rolling Characteristics

Twist or a combination of twist and camber produced only minor changes in the values of C_{Y_p}, C_{n_p}, and C_{l_p} at low and high lift coefficients but produced large changes in these derivatives at moderate lift coefficients (fig. 11) where the flow over the wings is changing from potential to separated flow. The small effects of twist and camber on C_{n_p} at low lift coefficients may be significant with regard to the lateral dynamic stability of an airplane. A combination of twist

and camber extended the initial linear range of C_{Y_p} and C_{n_p}. The linear range of these derivatives is generally smaller than that indicated by the curves of $C_D - \frac{C_L^2}{\pi A}$ (fig. 6) or the linear range of C_{l_β}, probably as a result of a higher angle of attack on the descending tip of the rolling wing. Camber increased the damping in roll slightly at low lift coefficients but caused a rapid decrease at about $C_L = 0.25$, which can be associated with the decrease in C_{L_α} that occurs at approximately the same lift coefficient. (See fig. 5.) At high lift coefficients, camber increased the damping in roll.

The increments in the rolling derivatives at moderate lift coefficients due to twist or camber are considerably larger than the increments caused by the addition of any one of several vertical tails to a wing-fuselage combination having the same wing as wing 1. (See ref. 6.)

Yawing Characteristics

Twist and camber produced changes in the yawing derivatives (fig. 12) unlike those produced in the rolling derivatives (fig. 11). Twist or camber produced large changes in the rolling derivatives only at moderate lift coefficients, whereas, for yawing derivatives, twist or camber produced essentially constant increments in the yawing derivatives throughout the lift-coefficient range.

The changes in C_{Y_r} caused by twist or camber are probably insignificant when the dynamic stability of an airplane is being considered; however, the changes in C_{n_r} and C_{l_r} due to twist or camber may be significant. The increments in C_{l_r} due to twist or camber in the moderate lift-coefficient range are greater than the increments produced by adding any one of several vertical tails to a wing-fuselage combination having a wing the same as wing 1 (ref. 7). Neither twist nor camber extended the linear part of the curve of C_{l_r} plotted against C_L; however, at higher Reynolds numbers, twist or camber, or both, might have larger effects on the linear part of the curve.

CONCLUSIONS

An investigation at low scale made in the Langley stability tunnel to determine the effect of linear spanwise variations of twist and circular-arc camber on the low-speed aerodynamic characteristics and

static- and rotary-stability derivatives of a wing with 45° sweepback of the quarter-chord line, an aspect ratio of 4, and a taper ratio of 0.6 led to the following conclusions:

1. Twist or camber produced only small changes in the maximum lift coefficient. A combination of camber and twist was more effective than twist alone in providing an increase in the maximum lift-to-drag ratio in the moderate lift-coefficient range.

2. The variation of static longitudinal stability through the lift-coefficient range was less for the twisted wing than for the plane wing or the twisted and cambered wing.

3. A combination of twist and camber generally extended the initial linear range of several of the static- and rotary-stability derivatives to a higher lift coefficient and, although these effects were rather small, higher Reynolds numbers may result in larger effects.

Langley Aeronautical Laboratory,
National Advisory Committee for Aeronautics,
Langley Field, Va., June 18, 1952.

REFERENCES

1. Campbell, John P., and Goodman, Alex: A Semiempirical Method for Estimating the Rolling Moment Due to Yawing of Airplanes. NACA TN 1984, 1949.

2. Toll, Thomas A., and Queijo, M. J.: Approximate Relations and Charts for Low-Speed Stability Derivatives of Swept Wings. NACA TN 1581, 1948.

3. MacLachlan, Robert, and Letko, William: Correlation of Two Experimental Methods of Determining the Rolling Characteristics of Unswept Wings. NACA TN 1309, 1947.

4. Bird, John D., Jaquet, Byron M., and Cowan, John W.: Effect of Fuselage and Tail Surfaces on Low-Speed Yawing Characteristics of a Swept-Wing Model as Determined in Curved-Flow Test Section of Langley Stability Tunnel. NACA TN 2483, 1951. (Supersedes NACA RM L8G13.)

5. Queijo, M. J., and Wolhart, Walter D.: Experimental Investigation of the Effect of Vertical-Tail Size and Length and of Fuselage Shape and Length on the Static Lateral Stability Characteristics of a Model With 45° Sweptback Wing and Tail Surfaces. NACA Rep. 1049, 1951. (Supersedes NACA TN 2168.)

6. Wolhart, Walter D.: Influence of Wing and Fuselage on the Vertical-Tail Contribution to the Low-Speed Rolling Derivatives of Midwing Airplane Models With 45° Sweptback Surfaces. NACA TN 2587, 1951.

7. Letko, William: Effect of Vertical-Tail Area and Length on the Yawing Stability Characteristics of a Model Having a 45° Sweptback Wing. NACA TN 2358, 1951.

TABLE I

WING SECTION ORDINATES

[NACA 65A008 thickness distribution]

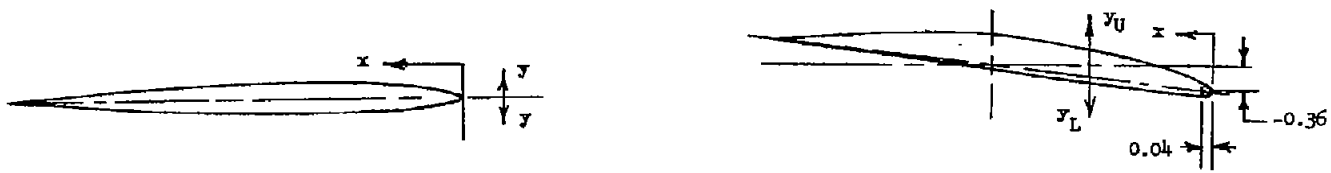

Root chord of wings 1, 2, and 3	
x, in.	y, in.
0	0
.056	.069
.084	.084
.141	.107
.281	.147
.563	.197
.844	.239
1.125	.274
1.688	.329
2.250	.371
2.813	.403
3.375	.427
3.938	.442
4.50	.449
5.063	.448
5.625	.438
6.188	.418
6.750	.389
7.313	.353
7.875	.311
8.438	.264
9.00	.214
9.563	.161
10.125	.108
10.688	.055
11.25	.002
L.E. rad. = 0.046 in.	

Tip chord of wings 1 and 2	
x, in.	y, in.
0	0
.034	.042
.051	.051
.085	.065
.170	.088
.340	.119
.510	.144
.680	.152
1.020	.199
1.36	.224
1.70	.244
2.04	.258
2.38	.267
2.72	.272
3.06	.271
3.40	.265
3.74	.252
4.08	.235
4.42	.214
4.76	.188
5.10	.160
5.44	.129
5.78	.097
6.12	.065
6.46	.033
6.80	.001
L.E. rad. = 0.028 in.	

Cambered tip chord of wing 3		
x, in.	y_U, in.	y_L, in.
0	-0.37	-0.37
.051	-.30	-.39
.085	-.275	-.41
.170	-.230	-.42
.340	-.175	-.42
.510	-.12	-.41
.680	-.07	-.39
1.020	.03	-.37
1.36	.12	-.34
1.70	.19	-.30
2.04	.26	-.27
2.38	.32	-.23
2.72	.375	-.18
3.06	.41	-.13
3.40	.44	-.08
3.74	.46	-.04
4.08	.47	.01
4.42	.47	.06
4.76	.475	.11
5.10	.47	.16
5.44	.45	.20
5.78	.43	.24
6.12	.41	.28
6.46	.38	.33
6.80	.37	.36
L.E. rad. = 0.04 in. x = 0.04, y = -0.36		

TABLE II

PERTINENT TEST DATA AND TEST CONDITIONS

Test	α, deg	β, deg	$\frac{pb}{2V}$	$\frac{rb}{2V}$	Mach number	Reynold's number
Static longitudinal	-2 to 32	0	0	0	0.17	0.895×10^6
Static lateral stability	-2 to 32	±2, ±5, ±8	0	0	.17	.895
	0, 8.2, 16.4	±2, ±5, ±8, ±12, ±16, ±20	0	0	.17	.895
Rolling	-2 to 32	0	±.019 ±.038 ±.056	0	.17	.895
Yawing	-2 to 32	0	0	0 -.031 -.066 -.087	.13	.707

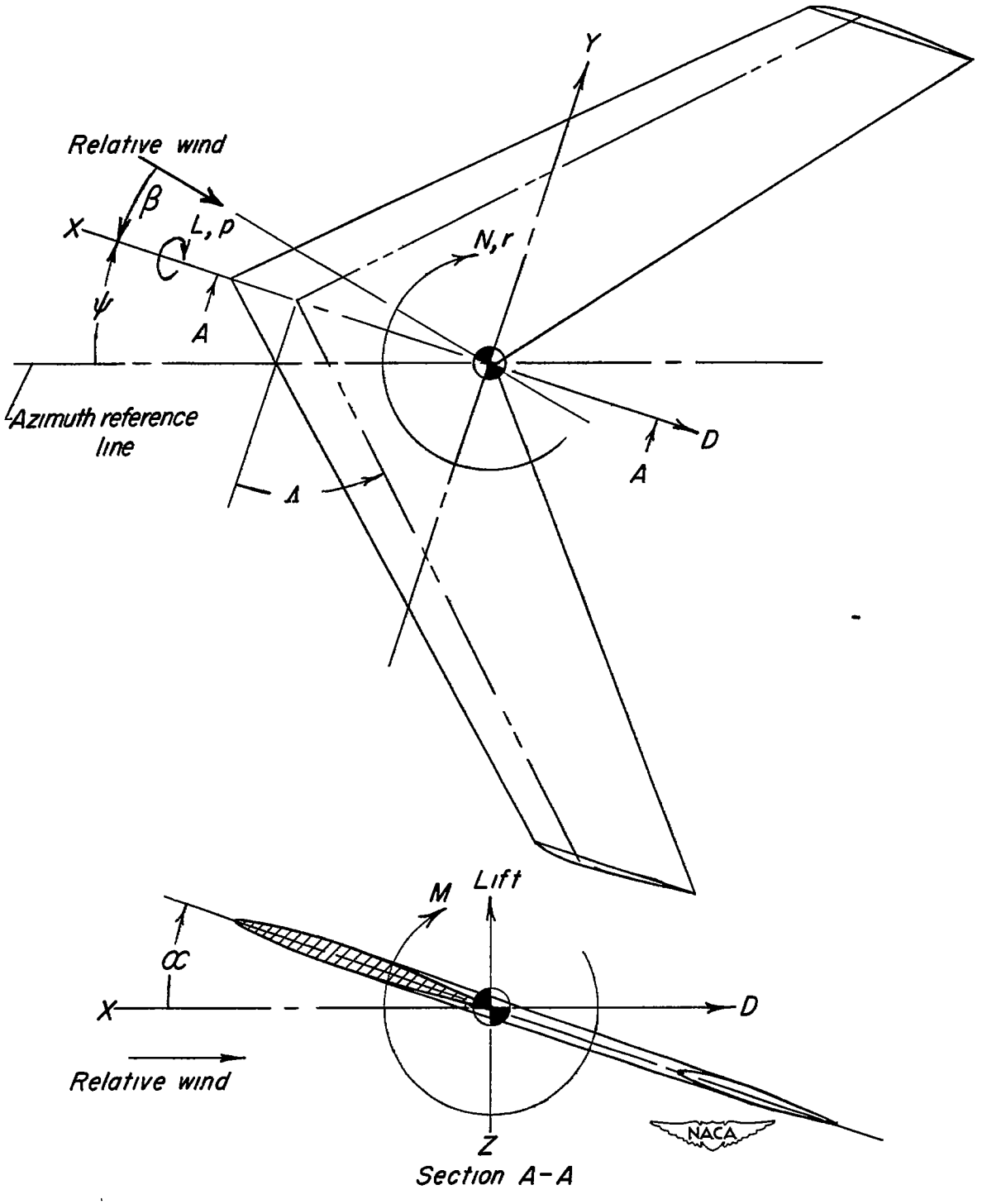

Figure 1.- System of stability axes. Arrows indicate positive directions of forces, moments, and angular displacements.

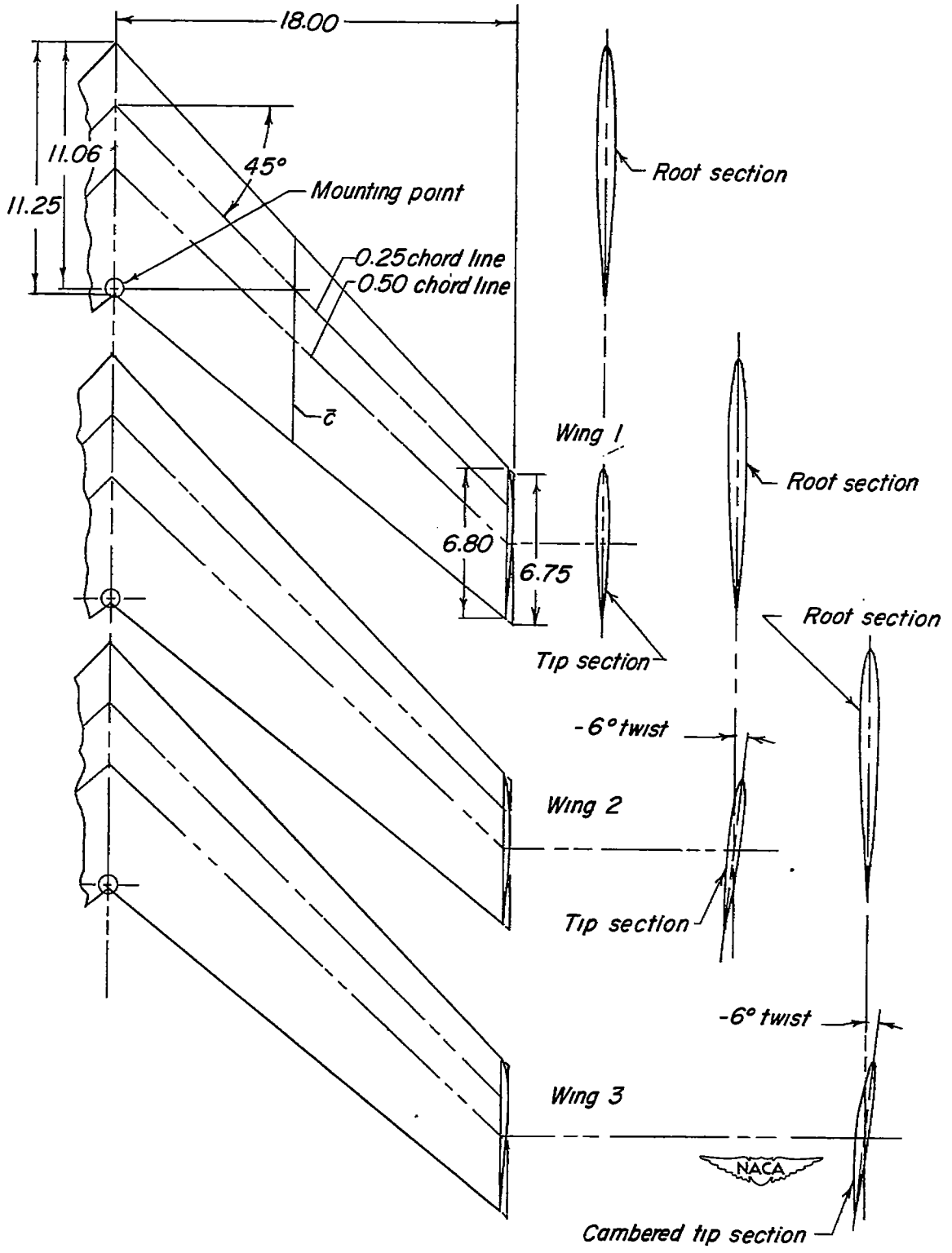

Figure 2.- Details of wings tested. All dimensions are in inches. A = 4; λ = 0.6; l = 324.0 square inches; $\bar{c}$ = 9.19 inches.

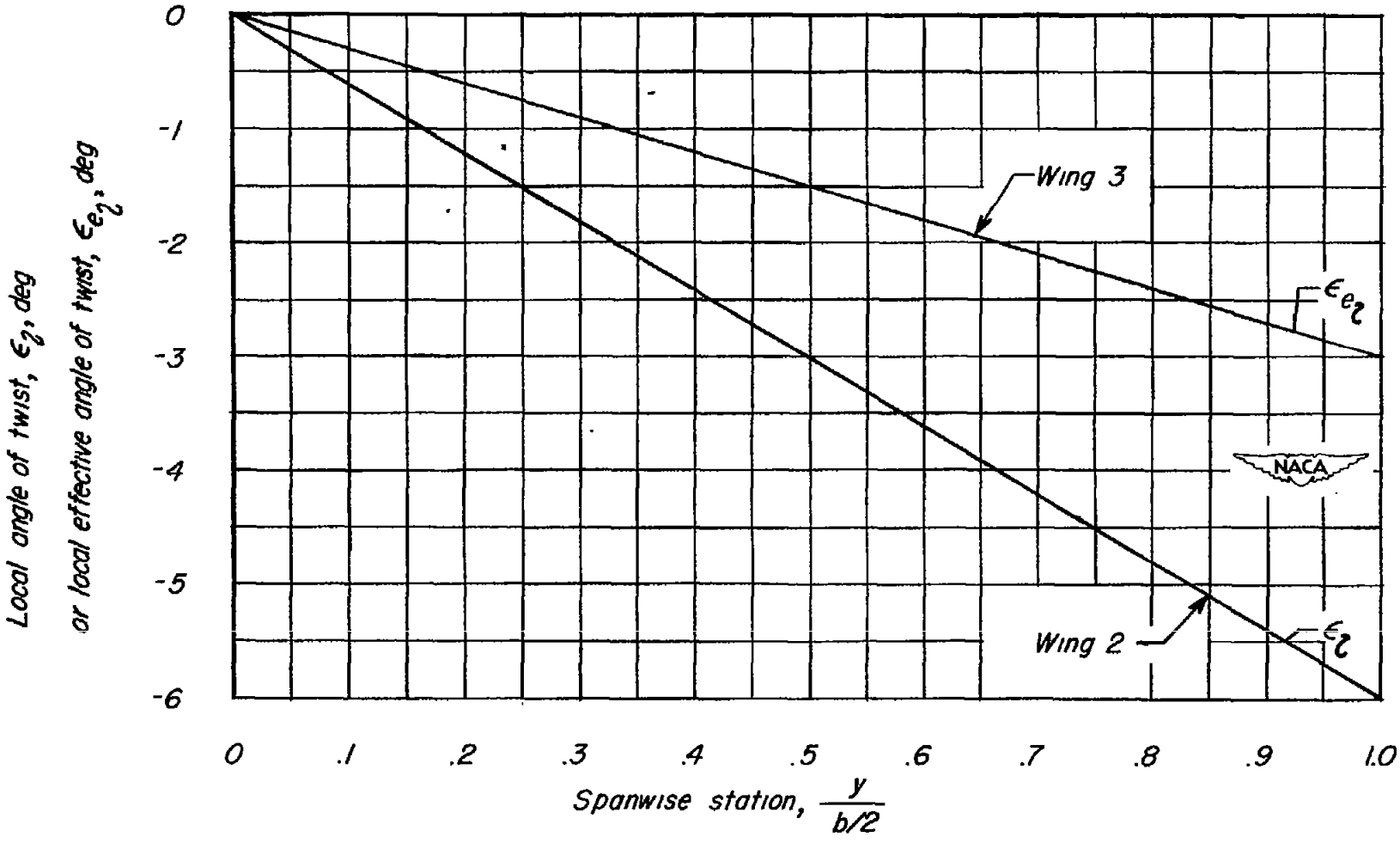

Figure 3.- Spanwise twist distribution for wings 2 and 3.

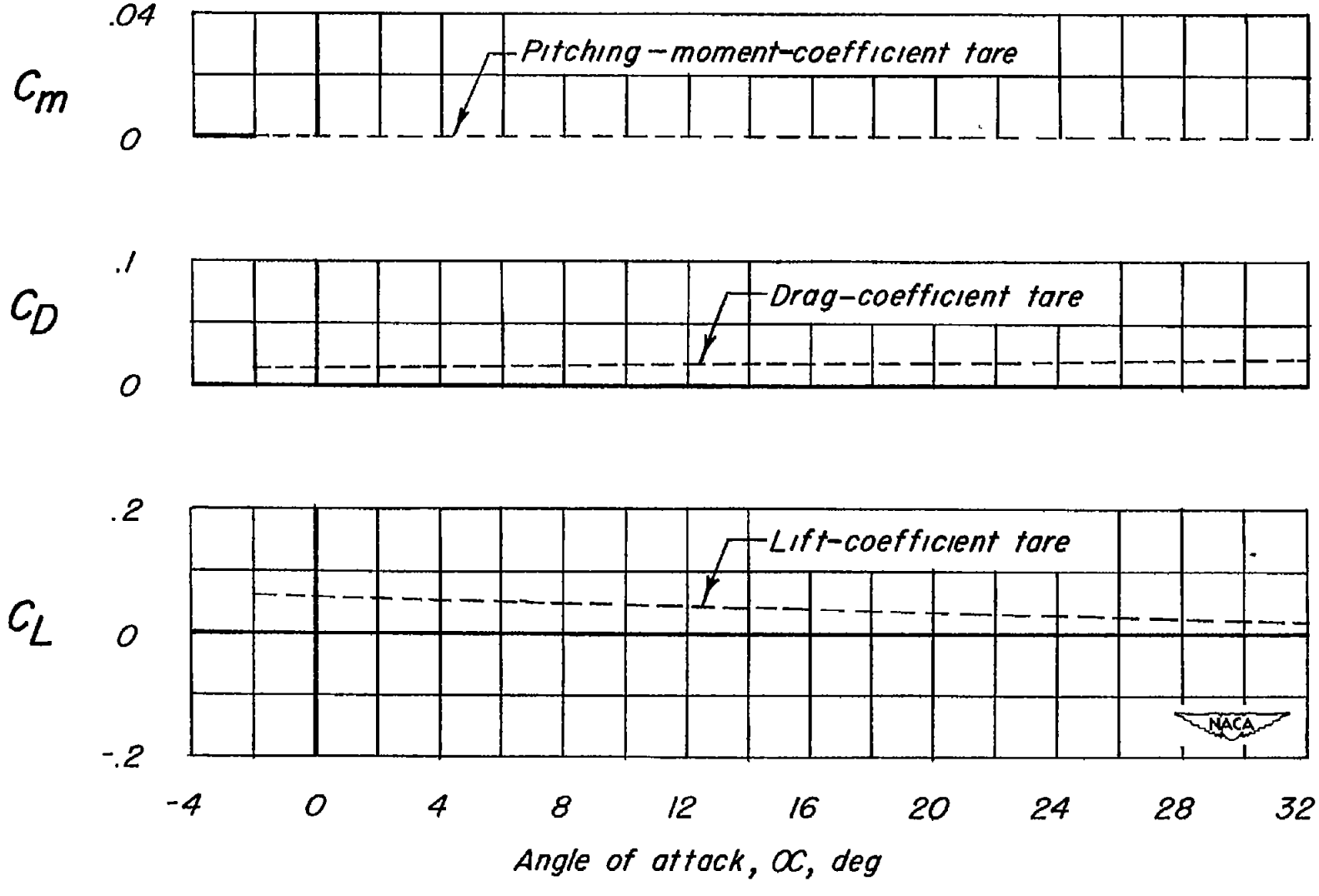

Figure 4.- Tares due to support strut used for the three wings.

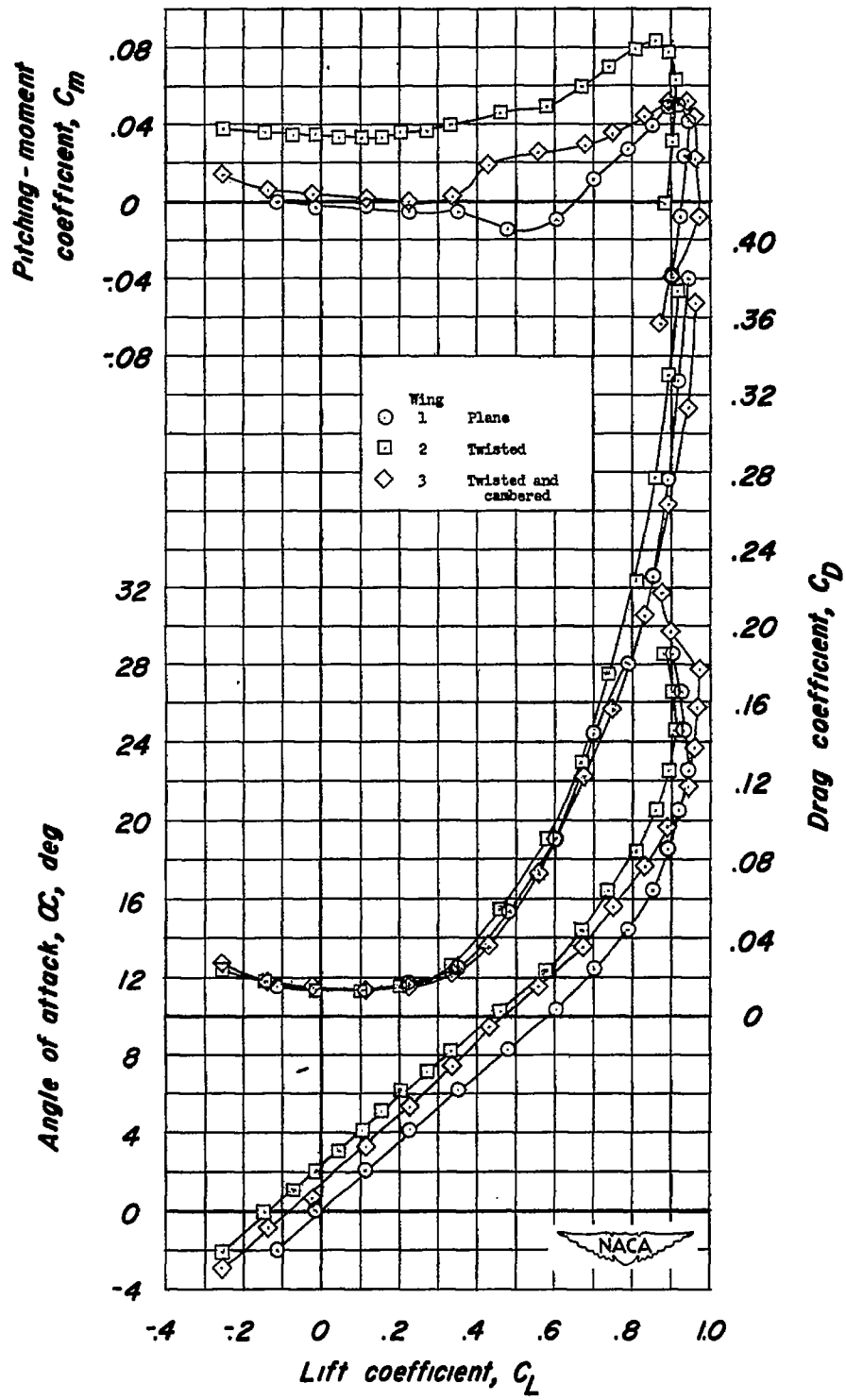

Figure 5.- Effects of twist and camber on variation of C_m, C_D, and α with C_L for a 45° sweptback wing of aspect ratio 4 and taper ratio 0.6. Reynolds number = 0.895×10^6; Mach number = 0.17; transition strips off.

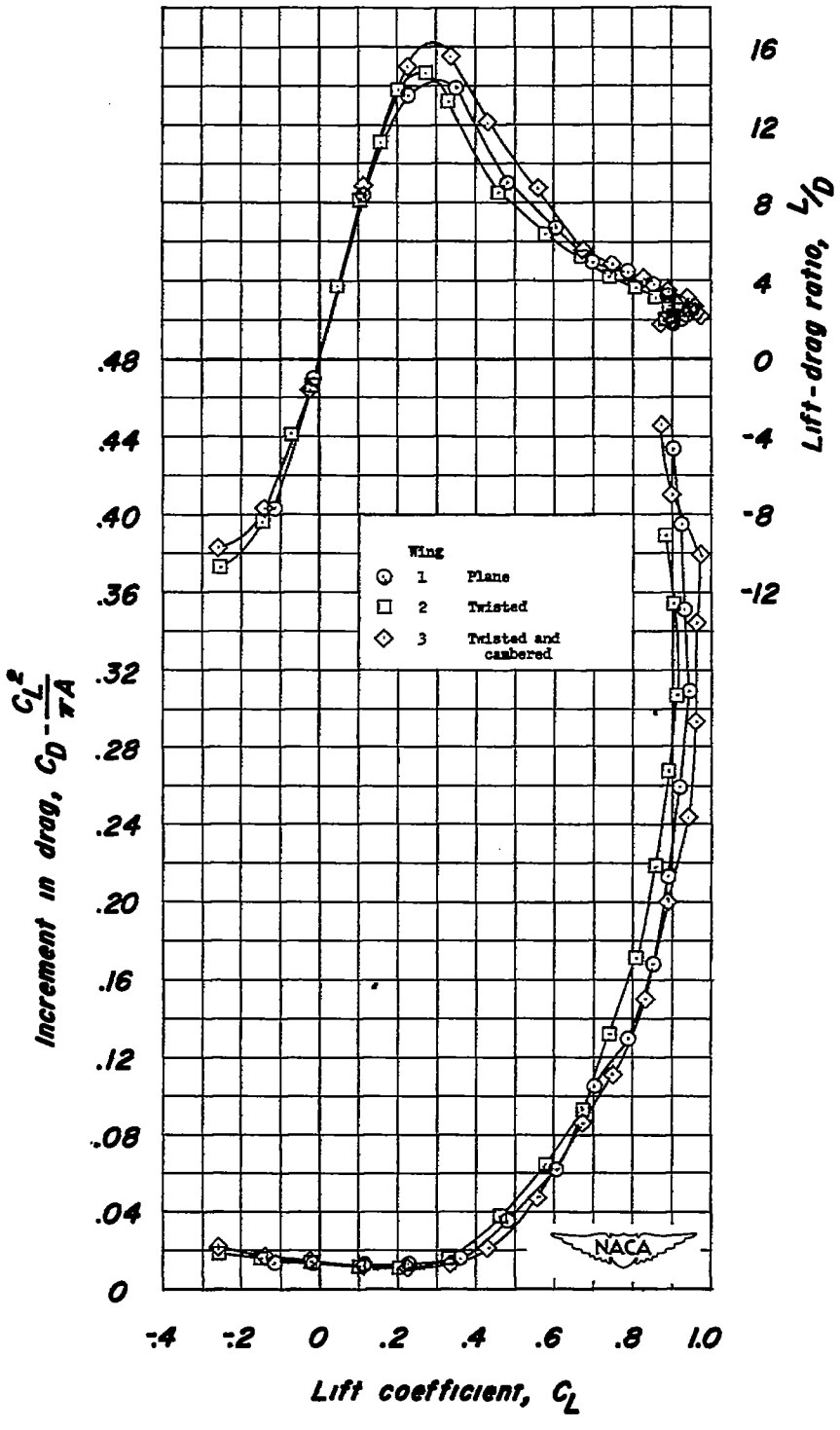

Figure 6.- Effects of twist and camber on variation of L/D and $C_D - \frac{C_L^2}{\pi A}$ with C_L for a 45° sweptback wing of aspect ratio 4 and taper ratio 0.6. Reynolds number = 0.895×10^6; Mach number = 0.17; transition strips off.

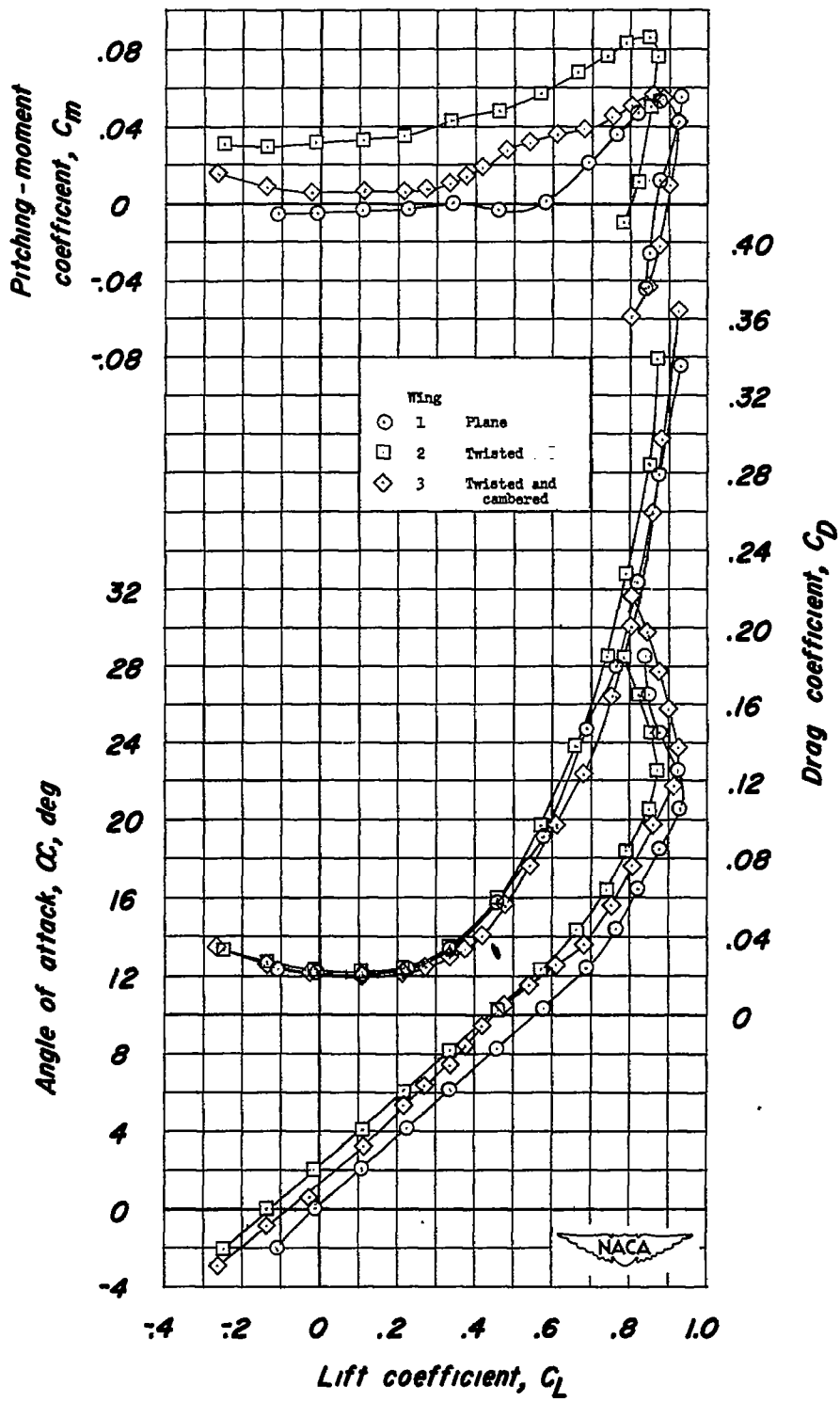

Figure 7.- Effects of twist and camber on variation of C_m, C_D, and α with C_L for a 45° sweptback wing of aspect ratio 4 and taper ratio 0.6. Reynolds number = 0.895×10^6; Mach number = 0.17; transition strips on.

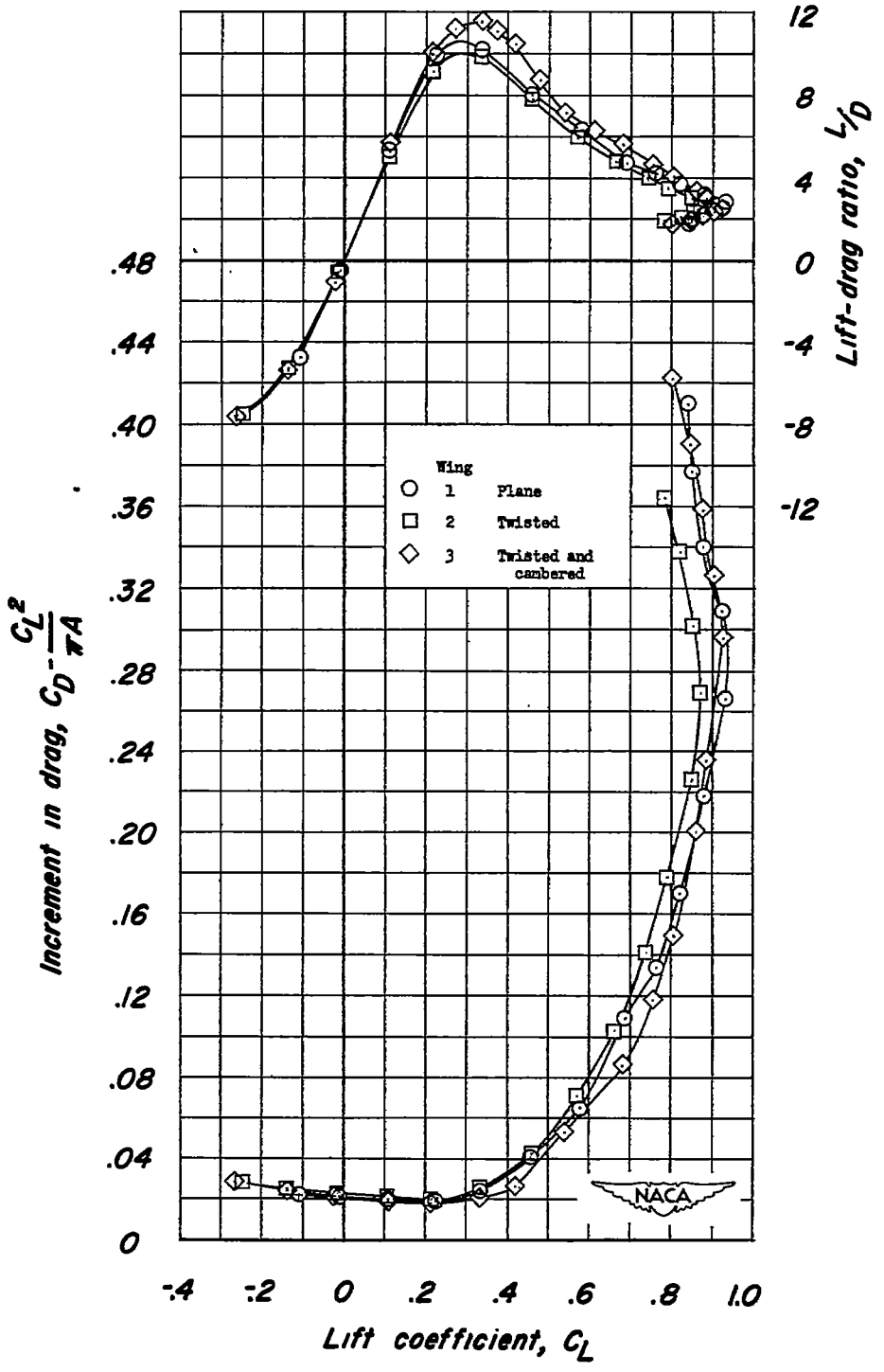

Figure 8.- Effects of twist and camber on variation of L/D and $C_D - \frac{C_L^2}{\pi A}$ with C_L for a 45° sweptback wing of aspect ratio 4 and taper ratio 0.6. Reynolds number = 0.895×10^6; Mach number = 0.17; transition strips on.

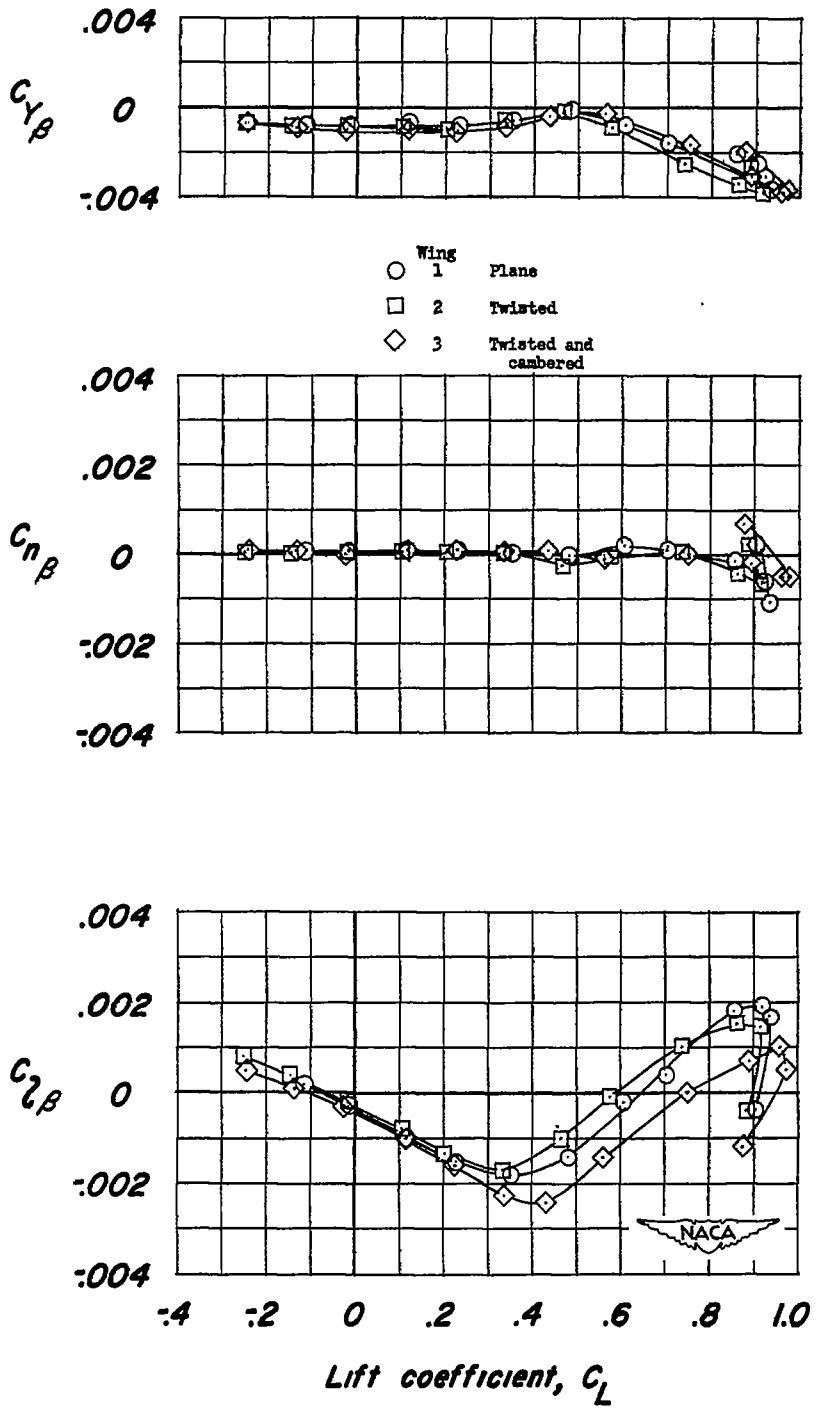

Figure 9.- Effects of twist and camber on variation of C_{Y_β}, C_{n_β}, and C_{l_β} with C_L for a 45° sweptback wing of aspect ratio 4 and taper ratio 0.6. Reynolds number = 0.895×10^6; Mach number = 0.17; transition strips off.

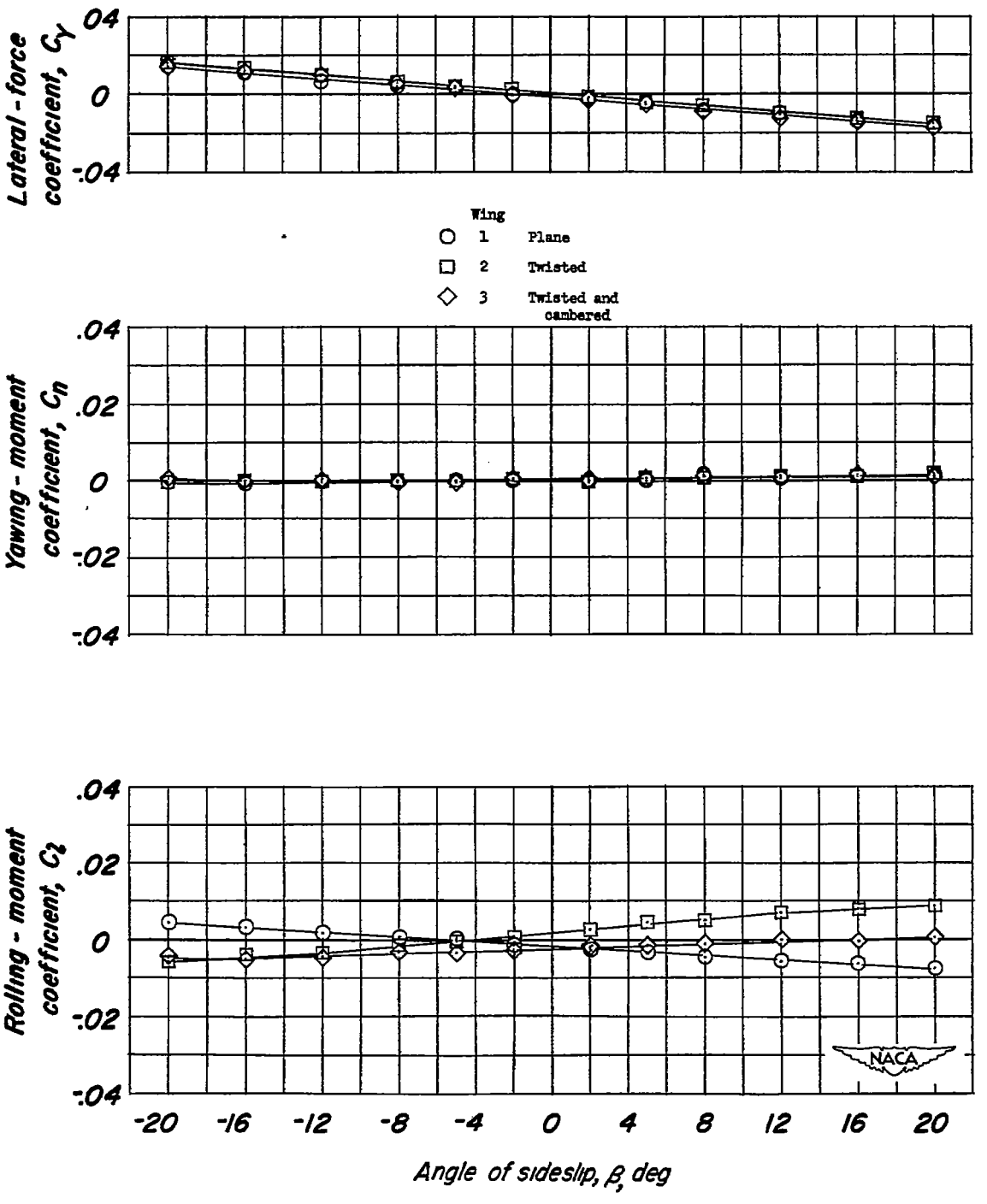

(a) $\alpha = 0^\circ$.

Figure 10.- Effects of twist and camber on variation of C_Y, C_n, and C_l with β for a 45° sweptback wing of aspect ratio 4 and taper ratio 0.6. Reynolds number = 0.895×10^6; Mach number = 0.17; transition strips off.

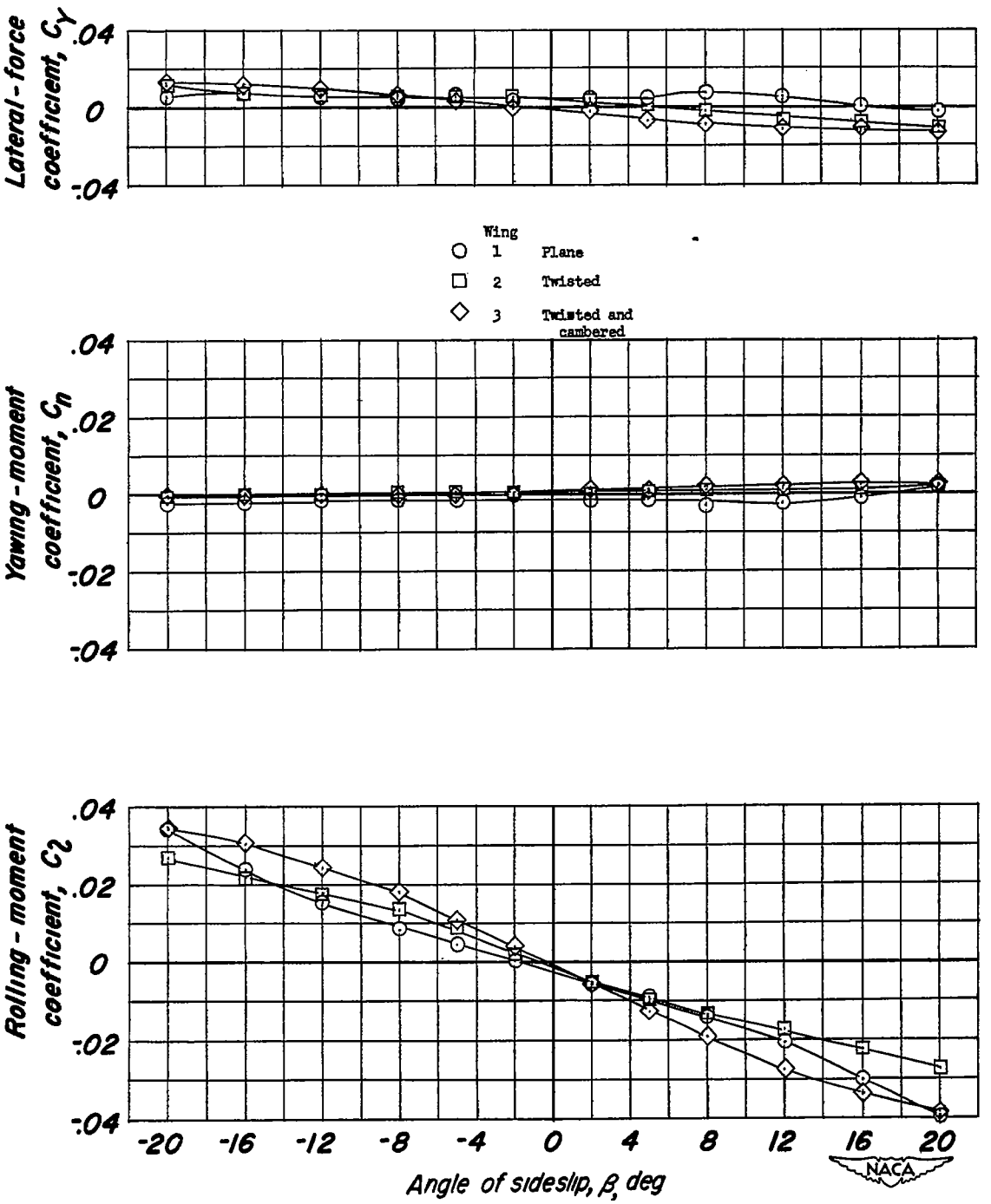

(b) $\alpha = 8.2^\circ$.

Figure 10.- Continued.

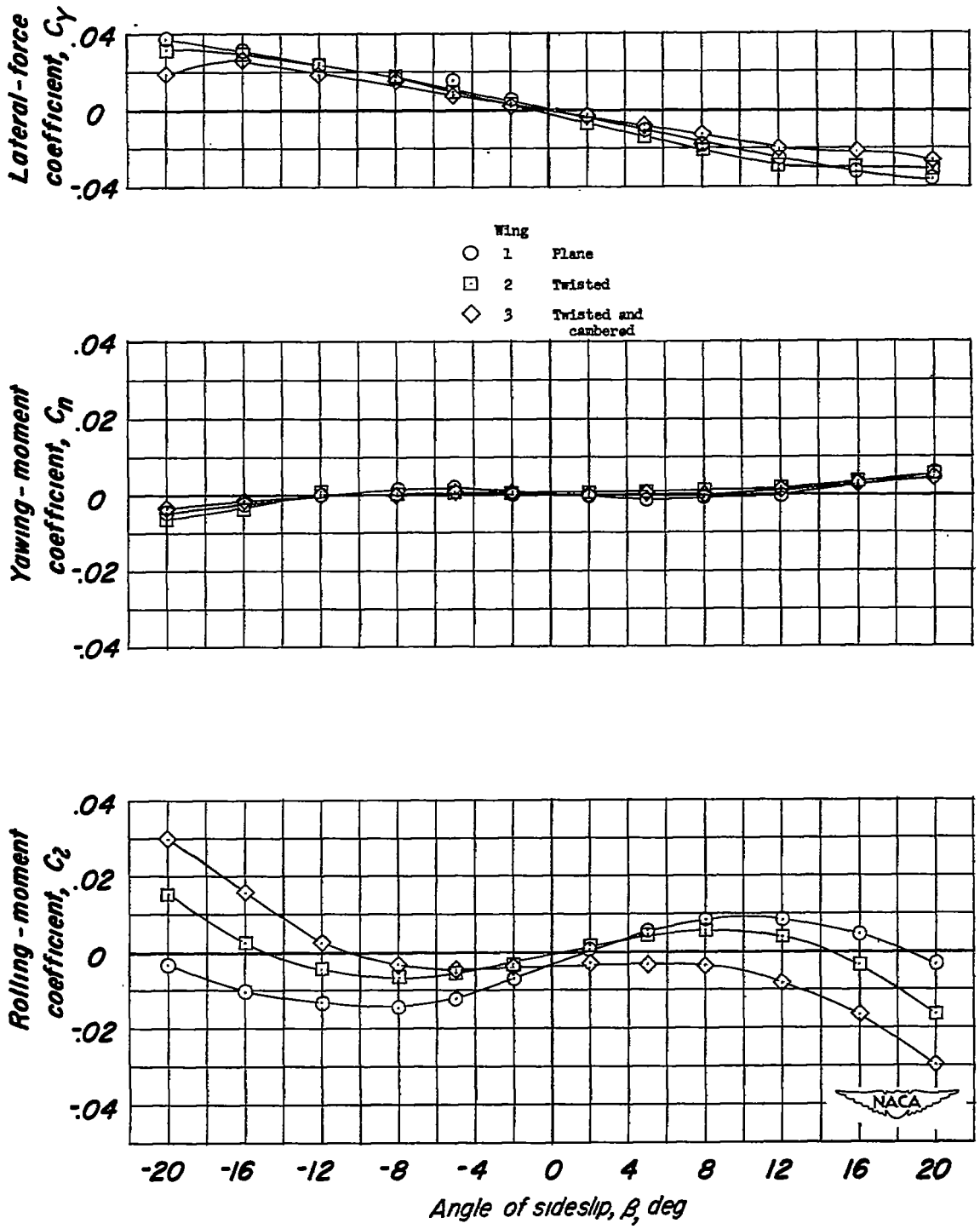

(c) $\alpha = 16.4^\circ$.

Figure 10.- Concluded.

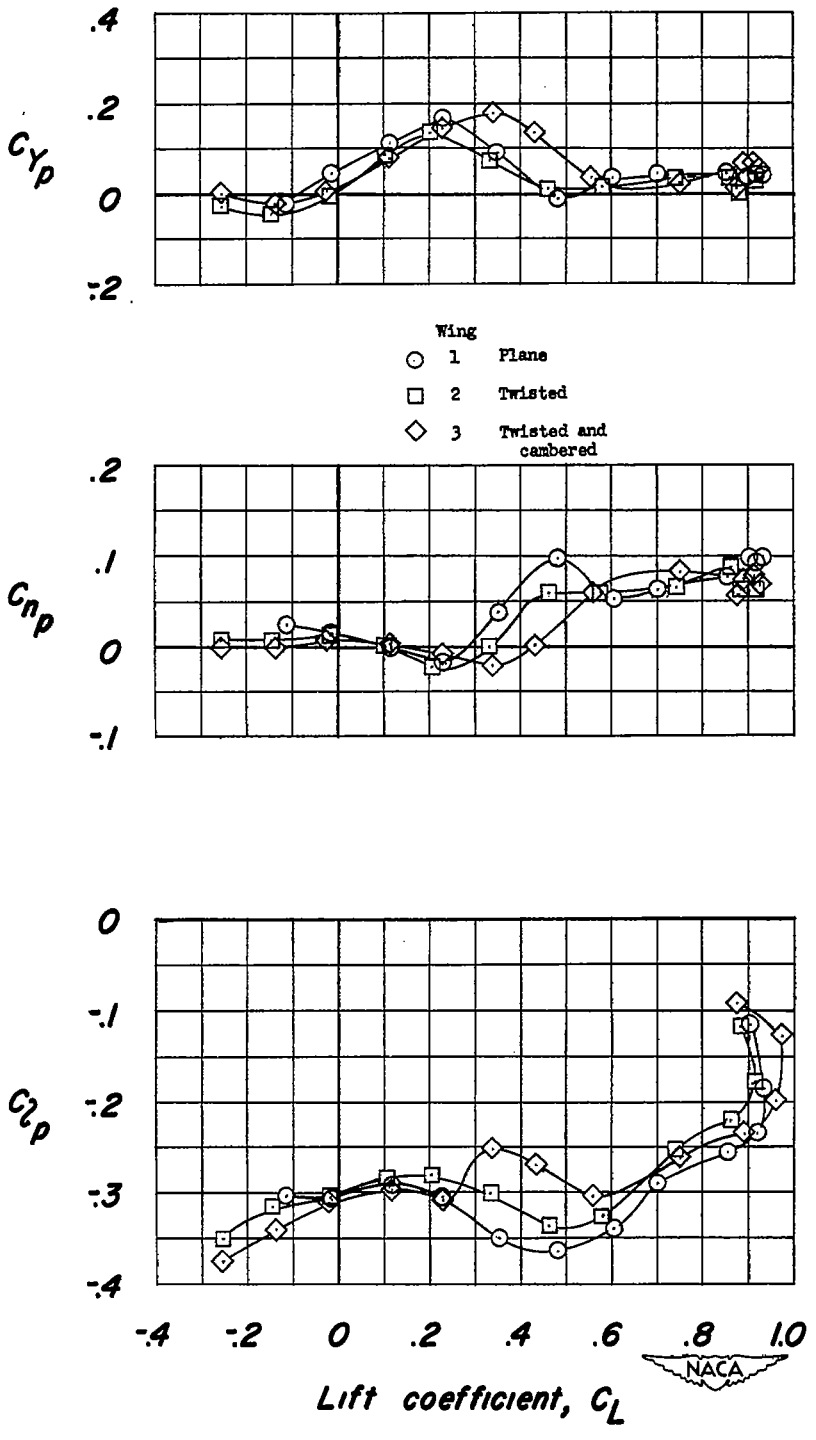

Figure 11.- Effects of twist and camber on variation of C_{Y_p}, C_{n_p}, and C_{l_p} with C_L for a 45° sweptback wing of aspect ratio 4 and taper ratio 0.6. Reynolds number = 0.895×10^6; Mach number = 0.17; transition strips off.

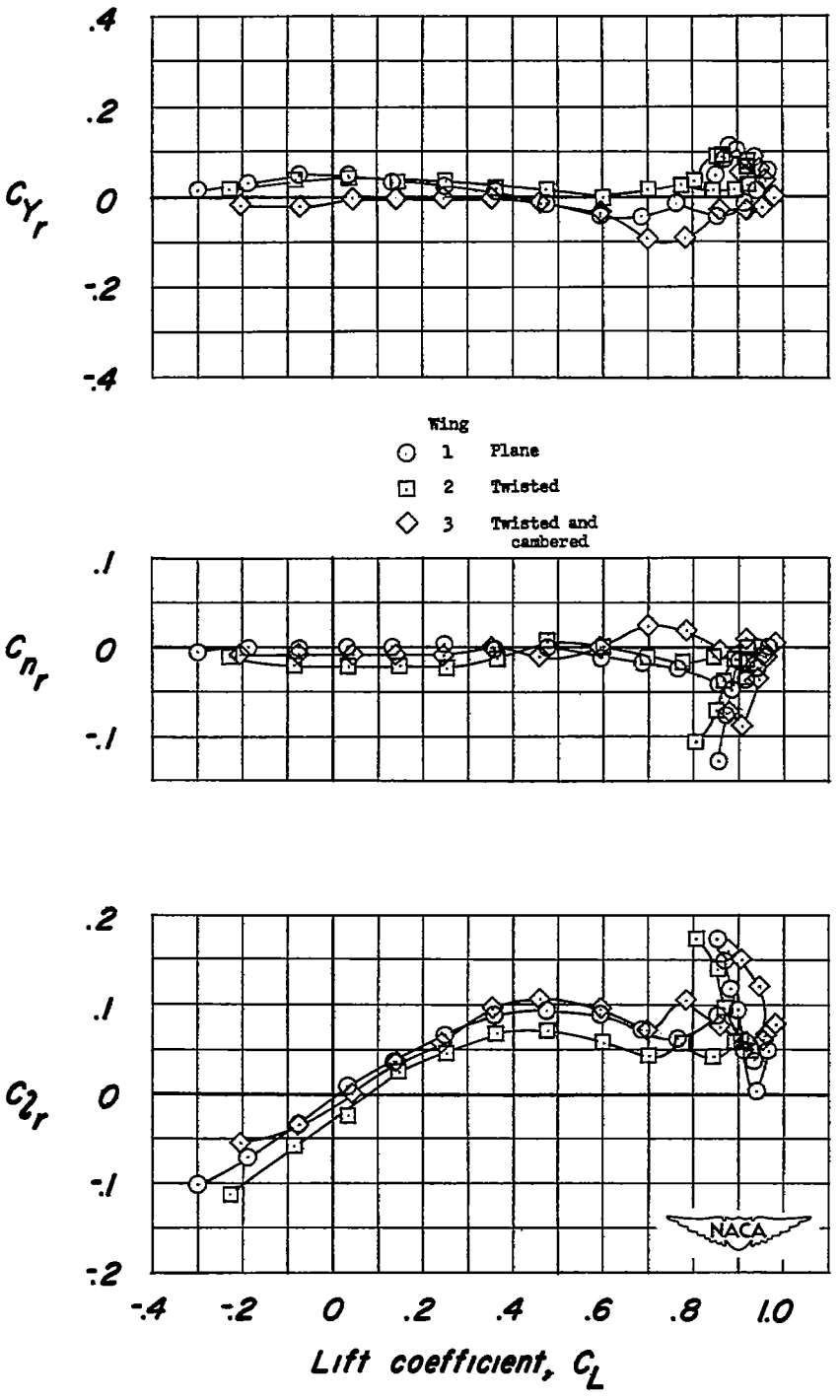

Figure 12.- Effects of twist and camber on variation of C_{Y_r}, C_{n_r}, and C_{l_r} with C_L for a 45° sweptback wing of aspect ratio 4 and taper ratio 0.6. Reynolds number = 0.707×10^6; Mach number = 0.13; transition strips off.

NACA-Langley - 8-27-52 - 1000